Human Motion Prediction on the IKEA-ASM Dataset

Mattias Billast[1][a], Kevin Mets[2][b], Tom De Schepper[1][c], José Oramas[1][d] and Steven Latré[1][e]
[1]*University of Antwerp - imec, IDLab, Department of Computer Science, Sint-Pietersvliet 7, 2000 Antwerp, Belgium*
[2]*University of Antwerp - imec, IDLab, Faculty of Applied Engineering, Sint-Pietersvliet 7, 2000 Antwerp, Belgium*

Keywords: Motion Prediction, Graph Neural Network, IKEA-ASM.

Abstract: Motion prediction of the human pose estimates future poses based on the preceding poses. It is a stepping stone toward industrial applications, like human-robot interactions and ergonomy indicators. The goal is to minimize the error in predicted joint positions on the IKEA-ASM dataset which resembles assembly use cases with a high diversity of execution and background of the same action class. In this paper, we use the STS-GCN model to tackle 2D motion prediction and make various alterations to improve the performance of the model. First, we pre-processed the training dataset through filtering to remove outliers and inconsistencies to boost performance by 31%. Secondly, we added object gaze information to give more context to the body motion of the subject, which lowers the error (MPJPE) to 10.1618 compared to 18.3462 without object gaze information. The increased performance indicates that there is a correlation between the object gaze and body motion. Lastly, the over-smoothing of the Graph Convolutional Network embeddings is decreased by limiting the number of layers, providing richer joint embeddings.

1 INTRODUCTION

Motion prediction of the human pose estimates future poses based on the preceding poses. Prediction in the spatial and temporal dimensions is a challenging task that has multiple purposes. The overall goal is to improve human-robot interactions, determine ergonomy indicators and increase safety. A possible use case is that users get an alert in a VR/AR setup when they are getting too close to a safety zone or when their posture is not ergonomic for long assembly tasks. The human pose is represented by a graph connecting 17 body joints. Typically, the time and space domains are modeled separately in human pose motion prediction. The time domain can be modeled with Recurrent Neural Networks (RNN), Long Short-Term Memory networks (LSTM), Gated Recurrent Unit (GRU), and recently with Transformers. The joint coordinates and their interactions are rather modeled with Graph Convolutional Networks (GCN). We opted for the STS-GCN model (Sofianos et al., 2021) as it models the space and time dimensions together as both dimensions are correlated while limiting cross-talk between the two. Both factors limit the number of parameters of the model, which enables fast real-time applications and the scalability of the model. The STS-GCN model is meant for 3D pose motion prediction but we repurposed it for 2D human pose motion prediction on the IKEA-ASM dataset (Ben-Shabat et al., 2020) for the first time. The goal is to upscale again in future work but the 2D case is a good subject to analyze alterations we made to the original dataset and model. 2D pose estimation models on RGB videos (He et al., 2017) are also more accurate than their 3D pose counterparts, as the depth dimension is difficult to estimate with only an RGB camera. All the models are trained on 2D pose estimations without manual annotations.
Our contributions are three-fold: first, we smooth the

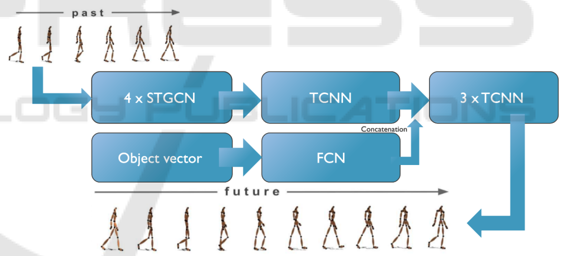

Figure 1: The STS-GCN-2D model architecture with added object information.

[a] https://orcid.org/0000-0002-1080-6847
[b] https://orcid.org/0000-0002-4812-4841
[c] https://orcid.org/0000-0002-2969-3133
[d] https://orcid.org/0000-0002-8607-5067
[e] https://orcid.org/0000-0003-0351-1714

Billast, M., Mets, K., De Schepper, T., Oramas, J. and Latré, S.
Human Motion Prediction on the IKEA-ASM Dataset.
DOI: 10.5220/0011902300003417
In *Proceedings of the 18th International Joint Conference on Computer Vision, Imaging and Computer Graphics Theory and Applications (VISIGRAPP 2023) - Volume 5: VISAPP*, pages 906-914
ISBN: 978-989-758-634-7; ISSN: 2184-4321

training dataset with simple filtering methods, to remove jumps and noise in the joint coordinates. Secondly, we add gaze context of the subject by including the object they are looking at or interacting with (shown in Figure 1 as object vector). Adding information about which object the subject is looking at, is also relevant in VR/AR use cases where there is egocentric data that can be added to the model and there is already work showing correlations between the active object and motion prediction (Zheng et al., 2022). Thirdly, we alter the number of GCN layers to minimize the over-smoothing effect on representations (Chen et al., 2020). Over-smoothing in a GCN occurs when there are too many layers and the nodes become indistinguishable from each other. This happens because, at each layer, a node is updated with an aggregate of neighboring nodes' feature vectors.

2 RELATED WORK

All recent human pose motion prediction uses deep learning models to leverage the motion patterns in the data.

Temporal Encoding. (Butepage et al., 2017) use Fully Connected Layers to temporally encode the inputs and decode them to look like the future outputs. Another temporal representation technique is RNN (Zhang et al., 2020) LSTM (Hu et al., 2019; Chiu et al., 2019), GRU (Yuan and Kitani, 2020; Adeli et al., 2020). These RNN models perform well but are difficult to train due to the vanishing/exploding gradient problem, and have millions of parameters (Gopalakrishnan et al., 2019) which require more data to train appropriately. The amount of parameters is also related to the number of computations, training time, and inference speed. Similar to an RNN, modeling the time domain with Transformers (Martínez-González et al., 2021; Vendrow et al., 2022) reports good results but also requires a lot of data. We opted for the Temporal Convolutional Layers (TCN) (Luo et al., 2018) as it is the state of the art with a relatively low amount of parameters.

Spatial Encoding. Regarding the spatial aspect, a Graph Convolutional Network (GCN) (Mohamed et al., 2021; Sofianos et al., 2021; Li et al., 2021; Liu et al., 2021) can represent the spatial interactions between joints in a natural way. The adjacency matrices can be handcrafted in the shape(Li et al., 2021) of the human pose or they can be trained iteratively by allowing connections between all nodes(Sofianos et al., 2021).

IKEA-ASM. To the best of our knowledge, motion prediction on the IKEA-ASM (Ben-Shabat et al., 2020) dataset has not been done. Most of the work on this dataset considers action recognition (Zhao et al., 2022), action segmentation (Ghoddoosian et al., 2022), and video alignment (Haresh et al., 2021; Kwon et al., 2022). The most recent work on this dataset (Diller et al., 2022) tackles action recognition and shows that characteristic poses of actions and the action labels are strongly correlated, which supports the use of context information when predicting poses.

3 METHODOLOGY

3.1 Problem Formulation

Motion prediction estimates the 2D coordinates of V joints for K frames given the previous T frames with V joints' coordinates as input. The goal is to minimize the Mean Per Joint Positional Error (MPJPE) of the estimated joint coordinates and their ground truths. The following equation gives the MPJPE:

$$MPJPE = \frac{1}{VK}\sum_{k=1}^{K}\sum_{v=1}^{V}\|\hat{x}_{vk} - x_{vk}\|_2 \quad (1)$$

where $\hat{x}_{vk}$ and x_{vk} are respectively the predicted coordinates and the ground truth coordinates of joint v at time k.

3.2 STS-GCN

For all the experiments, the STS-GCN model (Sofianos et al., 2021) is used. It consists of Spatio-Temporal Graph Convolutional layers (STGCN) followed by Temporal convolutional layers (TCNN), see Figure 1. The STGCN layers allow full space-space and time-time connectivity but limit space-time connectivity by replacing a full adjacency matrix with the multiplication of space and time adjacency matrices. The obtained feature embedding of the graph layers is decoded by four TCN layers which produce the forecasted human pose trajectories.

The motion trajectories in a typical GCN model are encoded into a graph structure with VT nodes for all body joints at each observed frame in time. The edges of the graph are defined by the adjacency matrix $A^{st} \in \mathbb{R}^{VT\times VT}$ in the spatial and temporal dimensions. The information is propagated through the network with the following equation:

$$H^{(l+1)} = \sigma(A^{st-(l)}H^{(l)}W^{(l)}) \quad (2)$$

where $H^{(l)} \in \mathbb{R}^{C^{(l)}\times V\times T}$ is the input to GCN layer l with $C^{(l)}$ the size of the hidden dimension which is

2 for the first layer, $W^{(l)} \in \mathbb{R}^{C^{(l)} \times C^{(l+1)}}$ are the trainable graph convolutional weights of layer l, σ the activation function and $A^{st-(l)}$ is the adjacency matrix at layer l.
The STS-GCN model alters the GCN model by replacing the adjacency matrix with the multiplication of T distinct spatial and V distinct temporal adjacency matrices.

$$H^{(l+1)} = \sigma(A^{s-(l)} A^{t-(l)} H^{(l)} W^{(l)}) \quad (3)$$

where $A^{s-(l)} \in \mathbb{R}^{V \times V}$ describes the joint-joint relations for each of T timesteps and $A^{t-(l)} \in \mathbb{R}^{T \times T}$ describes the time-time relations for each of V joints. This version limits the space-time connections and reports good performance (Sofianos et al., 2021). It lowers the number of parameters needed which is an advantage for real-time applications as it decreases inference speed. The trainable adjacency matrices with full joint-joint and time-time connections have attention properties as some nodes/timeframes will be more important for the predicted motion. Signed and directed graphs contain richer information to represent a larger variation of embeddings. In other words, the adjacency matrix can be asymmetrical with positive and negative weights. These negative weights have opposite semantic meaning, so a node can be affected by another node in two opposite ways which create greater variation.

3.3 Object Information

The idea to use gaze information is explored in Zheng et al. (Zheng et al., 2022) and shows great potential. We can hypothesize that the objects the subject is looking at and interacting with, are correlated with the motion trajectories. We add the context information into the model by concatenating an encoded object vector v_{oe} of the object that the subject is currently looking at with the feature embeddings after one TCNN layer. The concatenation of object vector and TCNN feature embeddings is shown in Figure 1. The added input information is ”oracle” data as we have the annotated action descriptions, which contain the objects the subject is interacting with. All (T+K) frames are sampled from the same action in all experiments to have one action description per sample. The object vector $v_o \in \mathbb{R}^{d \times a}$ is unique depending on the objects in the action class description of the sample, with d the maximum number of active objects together in the scene and a the number of possible objects in the scene. The first dimension is 2 because there are a maximum of 2 objects in the action description and the second dimension is 12 as there are 12 distinct objects in the action descriptions. An example of multiple active objects is the description ”align leg screw with table thread” which alludes that the subject interacts with the leg and the table. The object vector is fed through a fully connected neural network layer (FCN) with Relu activation function and $K \times V$ output nodes. The output is then reshaped to $v_{oe} \in \mathbb{R}^{K \times 2 \times V}$ to be concatenated with the GCN embeddings. The weights of the FCN are trained together with the STS-GCN model and adapted based on the MPJPE loss function. Figure 1 shows a simplified version of the architecture.

3.4 Oversmoothing in 2D Case

The original STS-GCN model has 4 layers in the 3D case but we hypothesize that this over-smoothens the features of the graph network in the 2D case. The features are a weighted average of the neighboring nodes' features and in the 2D case, there is less information to discriminate between nodes. Oversmoothing in a GCN occurs when the maximum number of hops between two nodes on the graph is small. If this number is smaller than the number of layers, all nodes contain information about other nodes. At each layer, the joint is updated with an aggregate of neighboring joints' features. The over-smoothing can be measured with the Mean Average Distance metric (MAD) (Chen et al., 2020), which is the average cosine distance between the hidden representations of node pairs. By lowering the number of layers, the MAD value increases and the over-smoothing effect reduces.

3.5 Using Fewer Joints

The joints that are not occluded generate better pose estimates compared to occluded joints. The lower body joints are occluded behind a table in 50% of the videos (Ben-Shabat et al., 2020). We analyze the cases where only 2 (hands) and 13 (upper body) joints are used, to remove noisy data from the data. Figure 2 shows the different graph structures that are used as input, the kinematic tree with 2 joints (hands) is not visualized as it is just 2 nodes. The hands' case is also a first step towards VR/AR use cases with an egocentric view when the only visible joints are the hands.

4 IMPLEMENTATION DETAILS

All models use 4 TCN layers, but we vary between 2 and 4 STGCN layers. During training, a range of learning rates was tested and the range of 2×10^{-3} – 8×10^{-3} gave the best results. The batch size is 256

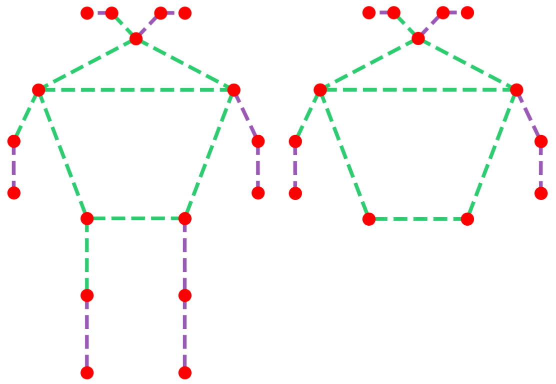

(a) (b)

Figure 2: Kinematic tree with (a) 17 and (b) 13 body joints.

for all experiments. To update the weights, an Adam optimizer is used with $\beta_1 = 0.9$, $\beta_2 = -.999$, and weight decay parameter $\lambda = 1 \times 10^{-5}$. The numbers of channels for the STGCN layers are respectively 3, 64, 32, and 64, and the number of channels for all four TCN layers is 25, equal to the output time frame. All models are trained for 50 epochs with a learning step scheduler which lowers the learning rate by a factor $\gamma = 0.1$ at epochs 15, 25, 35, and 40.

5 DATA

The dataset we used is the IKEA-ASM dataset which consists of 371 assembly videos with 48 unique subjects performing 33 action classes. There are in total around 3 million frames. Figure 5 shows the number of samples per action class in a logarithmic scale. The samples' distribution has a large influence on the results and generated outputs of the models. For example, the action "spin leg" is a predominant action in the dataset but only requires little motion to complete the action, i.e. turning of the wrist. Thus, models with a more static forecast are dominant. We chose the IKEA-ASM dataset because it is directly related to assembly use cases of motion prediction and has a high diversity of the same action class as the same furniture is assembled in a variety of ways with different backgrounds.

5.1 Data Filtering

All frames are annotated by a keypoint-rcnn model (He et al., 2017). This works most of the time, as can be seen in a qualitative example in Figure 4, but there are still jumps in the data when joints are occluded. Figure 3a shows some examples of the jumps in coordinates in the data for a single joint. To alleviate

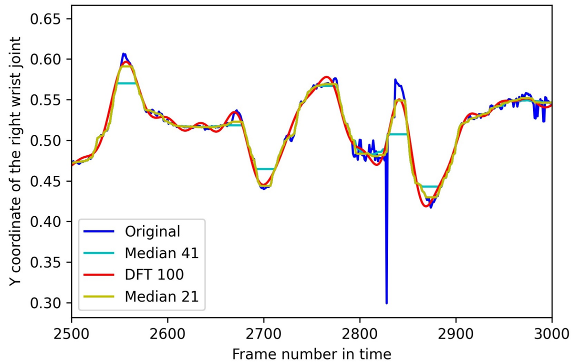

(a)

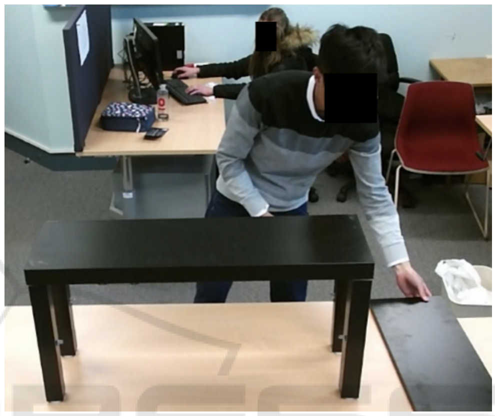

(b)

Figure 3: Data sample example: (a) the right wrist coordinates as a time series with various filters and (b) a snapshot at the frame when the jump in the time series occurs as the right wrist is occluded.

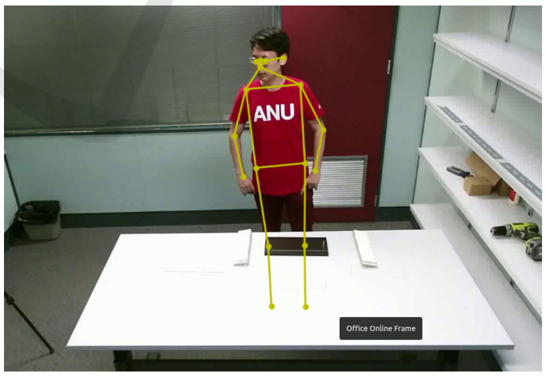

Figure 4: Qualitative example of human pose estimator to annotate data.

the problem of the high-frequency noisy data, multiple smoothing pre-processing methods are tested, i.e. a median filter (Justusson, 1981), and a discrete Fast Fourier Transform (DFT) lowpass filter (Nussbaumer, 1981). The DFT filter transforms the coordinate of the time series to the discrete frequency domain and only the first 100 frequencies (DFT 100) are used to

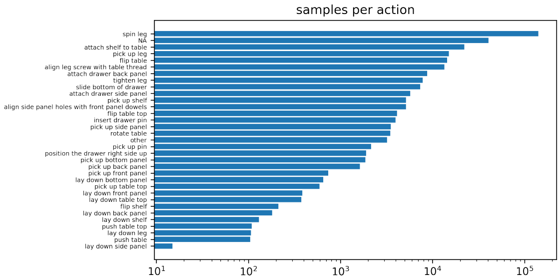

Figure 5: Distribution of actions in the IKEA-ASM dataset.

reconstruct the time series, thus removing the high-frequency oscillations. The median filter slides a window of size x over the time series and returns the median value within that window. Window sizes 21 (Median 21) and 41 (Median 41) are considered in the experiments. Figure 3a shows an example of each smoothing method and Figure 3b shows a frame when a jump in the right wrist coordinates' time series occurs.

6 RESULTS

In Tables 1, 2, 3, and 4, the MPJPE is listed for the various experiments. All experiments are done with 10 input frames and 25 predicted frames corresponding with a 1000ms prediction horizon. This setup is also used in most motion prediction benchmarks, allowing easy comparison with other methods. The results with the various modifications, i.e. data smoothing, adding object context, only using a part of the kinematic tree, and limiting the amount of STGCN layers are reported.

6.1 Baseline Results

To start, we implemented simple baseline predictions to have an indication of the relative performance. A first baseline is a static pose prediction where the last observed pose is the predicted pose throughout the prediction horizon. As many static actions exist in the dataset, the fixed position baseline works relatively well, as shown in Table 1. Other simple baselines like predicting the position of joints based on the average velocity, acceleration, and direction of the joints in the last 10 observed frames do not improve on the result of the fixed position baseline on the original dataset. This is mainly due to the outliers and inconsistencies in the data without pre-processing. These inconsistencies are mainly due to the differences in body joints' estimation of subsequent frames. The prediction based on the average velocity and acceleration is given by the following equation:

$$P_i = P_{input} + k_v \times v_{input} \times i + \frac{k_a \times a_{input} \times i^2}{2} \quad (4)$$

where P_i is the predicted pose at frame i, ranging from 1 to 25, P_{input} is the last pose of the input, k_v and k_a are the damping parameters, v_{input} is the average velocity of the input, and a_{input} is the average acceleration of the input.

6.2 Pre-Processing

We tested three different pre-processing filters, i.e. DFT 100, Median 21, and Median 41. The DFT 100 filter did smooth away outliers but introduced a sinusoidal wave pattern when the original joint coordinates remained constant. Other frequency cutoffs were considered but they either smoothed too much or too little. The median filter with a window of 41 (Median 41) smoothed away too much of the original data, while the median filter with a window of 21 (Median 21) performed best as it filtered outliers but still remained true to the original data when there is little noise.

6.2.1 Baselines

The baseline prediction, where a fixed velocity of the body joints is considered instead of a fixed position based on the input frames works better when validated on the smoothed dataset. Also including the average joints' acceleration in the observed frames, see Equation 4, improves the prediction even further on the smoothed dataset. An important note is that the average velocity and acceleration are damped with a factor k_v and k_a of 0.2 and 0.05 respectively as the predictions otherwise overshoot the actual movements for a horizon of 1000ms.

6.2.2 STS-GCN

In Table 1 the three data filters are examined together with the STS-GCN-2D model, i.e. DFT 100, Median 21, and Median 41. As shown in Table 1 the Median 41 filter worked best when the validation data was also smoothed but this could mean that the data is over-smoothed which is easier for a model to predict and does not give a fair comparison. Hence, all the validation data in subsequent experiments is the original un-processed data. When testing on the original data, using the Median 21 filter for training generalizes slightly better, so this filter is used for the next experiments. The sinusoidal wave the DFT 100 filter introduces, results in a jerky and periodic motion prediction of the joints and thus poor testing performance on the original data.

Table 1: MPJPE results of the baselines and adding various dataset smoothing methods.

Model	Nodes	#STGCN_L	Object	Data train filter	Data val filter	MPJPE
Fixed position	17	-	✗	-	Original	13.94
Fixed position	17	-	✗	-	Median 21	11.37
Fixed velocity	17	-	✗	-	Median 21	10.02
Fixed acceleration	17	-	✗	-	Median 21	9.7624
STS-GCN-2D	17	4	✗	Median 41	Median 41	8.1938
STS-GCN-2D	17	4	✗	Median 21	Median 21	9.9145
STS-GCN-2D	17	4	✗	DFT 100	DFT 100	9.7385
STS-GCN-2D	17	4	✗	Median 41	Original	12.8814
STS-GCN-2D	17	4	✗	Median 21	Original	**12.6363**
STS-GCN-2D	17	4	✗	DFT 100	Original	26.5258
STS-GCN-2D	17	4	✗	Original	Original	18.3462

Table 2: MPJPE results of the isolated improvements on the STS-GCN-2D model.

Model	Nodes	#STGCN_L	Object	Data train filter	Data val filter	MPJPE
Fixed position	17	-	✗	-	Original	13.94
STS-GCN-2D	17	4	✗	Original	Original	18.3462
STS-GCN-2D	17	4	✓	Original	Original	**10.1618**
STS-GCN-2D	17	2	✗	Original	Original	16.7893
STS-GCN-2D	13	4	✗	Original	Original	11.8570

6.3 Architecture Changes

Table 2 shows the results where various changes are applied to the STS-GCN-2D model.

6.3.1 Active Object Information

Adding object information does perform better than the model without object information, confirming the hypothesis that there is a correlation between the object the subject is interacting with and the joints' motion trajectories. Adding object context has the best overall MPJPE as there is a lot of added input information that is derived from the manually annotated action labels. In the future, an oracle can be replaced by an active object estimator which makes it more realistic.

6.3.2 Skeleton Configuration

Limiting the number of joints to 13 (upper body) to remove unnecessary or error-prone movement regarding the action task at hand improves the results compared to the model with 17 joints. The upper body has fewer occlusions than the lower body which is occluded behind a table for 50% of the videos. Following this reasoning, the joints' coordinates of the upper body are overall more accurate.

6.3.3 Minimizing Over-Smoothing GCN

Using two STGCN layers instead of four provides a small improvement for the simple 2D model on all joints. By only using 2 layers, the MAD value increased from 0.58 to 0.60. This is a marginal gain but it did translate to a small increase in performance on the testing data, as we compare row 2 and 4 in Table 2. A minimal increase in MAD value by lowering the number of layers to two indicates that there is less over-smoothing of the graph representation than with four layers.

6.3.4 Combining of Improvments

Table 3 shows the performance achieved by various combinations of the previously explained changes.

Active Object + Smoothing. The table shows that combining object context and training on smoothed dataset does not necessarily improve the results on the original dataset. A possible explanation might be that high-frequencies present in the original (non-smoothed) dataset give an indication of what motion is going to occur and combining with object context gives a good prediction.

Custom Skeleton Configuration + Smoothing. Limiting the number of joints to 13 (upper body) or 2 (hands) to remove unnecessary or error-prone movement regarding the action task at hand has different results. The case with 13 joints improves the results

Table 3: MPJPE results of the combinations of improvements on STS-GCN-2D model, while also including some baselines.

Model	Nodes	#STGCN_L	Object	Data train filter	Data val filter	MPJPE
Fixed position	17	-	✗	-	Original	13.94
STS-GCN-2D	17	4	✗	Original	Original	18.3462
STS-GCN-2D	17	4	✓	Original	Original	10.1618
STS-GCN-2D	17	4	✓	Median 21	Original	12.6789
STS-GCN-2D	13	4	✓	Median 21	Original	12.2306
STS-GCN-2D	13	2	✓	Median 21	Original	12.8616
STS-GCN-2D	2	4	✓	Median 21	Original	16.9668
STS-GCN-2D	2	2	✓	Median 21	Original	16.8866

Table 4: MPJPE results of various combinations of STS-GCN-2D model trained on the floor and table dataset splits.

	Nodes	#STGCN_L	Object	Data train filter	Data val filter	MPJPE
1	17	4	✓	Full split	Full split	10.1618
2	17	4	✓	Full split	Table split	10.1224
3	17	4	✓	Full split	Floor split	10.1845
4	13	4	✓	Full split	Full split	11.2891
5	13	4	✓	Full split	Table split	11.6197
6	13	4	✓	Full split	Floor split	11.0983
7	17	4	✓	Table split	Full split	17.5242
8	17	4	✓	Floor split	Full split	12.6189
9	13	4	✓	Table split	Full split	15.1431
10	13	4	✓	Floor split	Full split	12.8331
11	17	4	✓	Median21 Table split	Full split	15.5269
12	17	4	✓	Median21 Floor split	Full split	12.9247
13	13	4	✓	Median21 Table split	Full split	15.2879
14	13	4	✓	Median21 Floor split	Full split	12.9681

compared to the model with 17 joints. In the hands' case (2 joints), the results did not improve as there is too little information on the whole kinematic tree to make a correct motion prediction of only the hands.

Custom Skeleton Configuration + Smoothing + 2 STGCN Layers. On the other hand, using two STGCN layers has a factor when only considering the hands. The reasoning here would be that these 2 joints are over-smoothed as each layer outputs a weighted average of the neighboring joints. With 4 layers all the information of a specific node is vanished due to this smoothing effect. The MAD value increased from 0.484 with four layers to 0.729 with two layers which backs the hypothesis that there is significantly more over-smoothing with four layers. The hands' case with improvements still performed better than the original model with 17 joints and no improvements, which is a first indicator that VR/AR industrial use cases with motion prediction are feasible. This is a good result as the MPJPE gives a "per joint" error but when we only evaluate the hands' joints which are the joints with the most movement in an assembly task, it is difficult to compare the different settings. Following this reasoning, the hands' case is the most difficult setting to perform well.

Figures 6 and 7 show qualitative results of the predicted sequences of different actions by the STS-GCN model with object context, 2 STGCN layers, and trained on the smoothed dataset.

6.4 Occlusions

To examine the effect of occlusions, the dataset is split into two parts, one with a table in front of the subject and one without a table. Table 4 shows the results when only using these splits of the dataset, i.e. splits where there is respectively a table (Table split) or not (Floor split) in the assembly scene which can occlude the lower part of the body and increase the noise in the dataset. The models trained on the full data performed similarly on the original, table, and floor validation datasets. We can reason that the model is robust to the occluded data samples. On the other hand, the models trained on the floor dataset generalize much better to the full dataset than the models trained on the table dataset with occlusions. The largest improvement, when trained on the table split, is observed when 13 nodes instead of 17 are used and

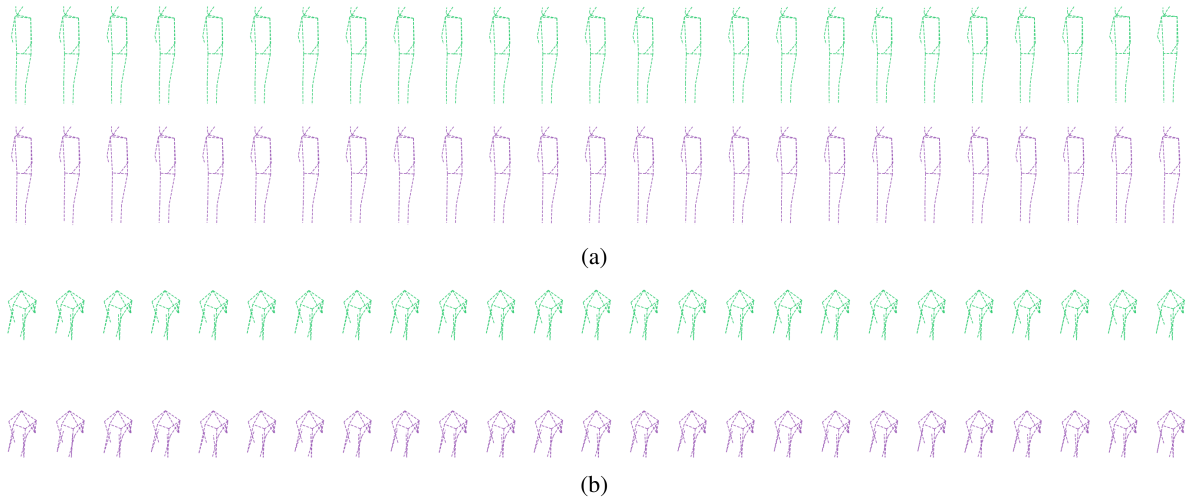

Figure 6: Separated prediction (purple) and ground truth (green) motion sequences of the action (a) ”spin leg’ and (b) ”attach drawer side panel” by the STS-GCN-2D model with object context, trained on the smoothed IKEA-ASM dataset.

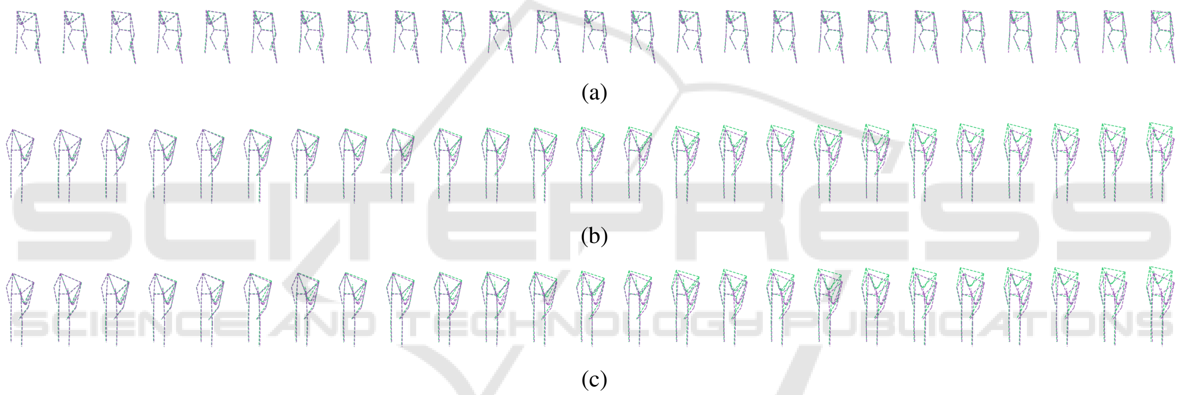

Figure 7: Prediction (purple) and ground truth (green) motion sequences of the action (a) ”spin leg’, (b) ”attach drawer side panel”, and (c) ”attach drawer side panel” by the STS-GCN-2D model with object context, trained on the smoothed IKEA-ASM dataset.

tested on the full dataset, which can be seen by comparing rows 7 and 9 in Table 4. Removing lower body joints from the training samples boosts the data quality. This improvement is diminished when the training set is filtered with a Median 21 filter because then the occluded lower body joint estimations are more accurate and actually add information to the model. With filtering, it is not opportune to remove the lower body joints as input.

7 CONCLUSION AND FUTURE WORK

We summarize our work on 2D motion prediction on the IKEA-ASM dataset by the following modifications to the dataset and model. Pre-processing the dataset to remove outliers and inconsistencies boosts performance. We added object gaze information to give more context to the body motion of the subject. Over-smoothing of the GCN embeddings is decreased by limiting the number of layers. Lastly, only using the upper body joints improves the results as the lower body pose estimations are error-prone.

Future work includes adding baselines mentioned in the related work section to have stronger comparisons. The object gaze information is currently added as an oracle but in certain use cases it is more realistic to predict the active object given the raw video inputs, this problem is tackled in one of the MECCANO dataset challenges (Ragusa et al., 2022). Adding an active object detector is one of the possible future directions that can be explored. With 3D human poses, it is also possible to constrain the possible joint trajectories with the physical constraints of the kinematic tree as there are accurate angles and distances between nodes in 3D.

ACKNOWLEDGEMENTS

This research received funding from the Flemish Government (AI Research Program).

REFERENCES

Adeli, V., Adeli, E., Reid, I., Niebles, J. C., and Rezatofighi, H. (2020). Socially and contextually aware human motion and pose forecasting. *IEEE Robotics and Automation Letters*, 5(4):6033–6040.

Ben-Shabat, Y., Yu, X., Saleh, F., Campbell, D., Rodriguez-Opazo, C., Li, H., and Gould, S. (2020). The ikea asm dataset: Understanding people assembling furniture through actions, objects and pose.

Butepage, J., Black, M. J., Kragic, D., and Kjellstrom, H. (2017). Deep representation learning for human motion prediction and classification. In *Proceedings of the IEEE conference on computer vision and pattern recognition*, pages 6158–6166.

Chen, D., Lin, Y., Li, W., Li, P., Zhou, J., and Sun, X. (2020). Measuring and relieving the over-smoothing problem for graph neural networks from the topological view. In *Proceedings of the AAAI Conference on Artificial Intelligence*, volume 34, pages 3438–3445.

Chiu, H.-k., Adeli, E., Wang, B., Huang, D.-A., and Niebles, J. C. (2019). Action-agnostic human pose forecasting. In *2019 IEEE Winter Conference on Applications of Computer Vision (WACV)*, pages 1423–1432. IEEE.

Diller, C., Funkhouser, T., and Dai, A. (2022). Forecasting actions and characteristic 3d poses. *arXiv preprint arXiv:2211.14309*.

Ghoddoosian, R., Dwivedi, I., Agarwal, N., Choi, C., and Dariush, B. (2022). Weakly-supervised online action segmentation in multi-view instructional videos. In *Proceedings of the IEEE/CVF Conference on Computer Vision and Pattern Recognition*, pages 13780–13790.

Gopalakrishnan, A., Mali, A., Kifer, D., Giles, L., and Ororbia, A. G. (2019). A neural temporal model for human motion prediction. In *Proceedings of the IEEE/CVF Conference on Computer Vision and Pattern Recognition (CVPR)*.

Haresh, S., Kumar, S., Coskun, H., Syed, S. N., Konin, A., Zia, Z., and Tran, Q.-H. (2021). Learning by aligning videos in time. In *Proceedings of the IEEE/CVF Conference on Computer Vision and Pattern Recognition*, pages 5548–5558.

He, K., Gkioxari, G., Dollar, P., and Girshick, R. (2017). Mask r-cnn. In *Proceedings of the IEEE International Conference on Computer Vision (ICCV)*.

Hu, J., Fan, Z., Liao, J., and Liu, L. (2019). Predicting long-term skeletal motions by a spatio-temporal hierarchical recurrent network. *arXiv preprint arXiv:1911.02404*.

Justusson, B. (1981). Median filtering: Statistical properties. *Two-Dimensional Digital Signal Prcessing II*, pages 161–196.

Kwon, T., Tekin, B., Tang, S., and Pollefeys, M. (2022). Context-aware sequence alignment using 4d skeletal augmentation. In *Proceedings of the IEEE/CVF Conference on Computer Vision and Pattern Recognition (CVPR)*, pages 8172–8182.

Li, Q., Chalvatzaki, G., Peters, J., and Wang, Y. (2021). Directed acyclic graph neural network for human motion prediction. In *2021 IEEE International Conference on Robotics and Automation (ICRA)*, pages 3197–3204. IEEE.

Liu, Z., Su, P., Wu, S., Shen, X., Chen, H., Hao, Y., and Wang, M. (2021). Motion prediction using trajectory cues. In *Proceedings of the IEEE/CVF International Conference on Computer Vision*, pages 13299–13308.

Luo, W., Yang, B., and Urtasun, R. (2018). Fast and furious: Real time end-to-end 3d detection, tracking and motion forecasting with a single convolutional net. In *Proceedings of the IEEE conference on Computer Vision and Pattern Recognition*, pages 3569–3577.

Martínez-González, A., Villamizar, M., and Odobez, J.-M. (2021). Pose transformers (potr): Human motion prediction with non-autoregressive transformers. In *Proceedings of the IEEE/CVF International Conference on Computer Vision*, pages 2276–2284.

Mohamed, A., Chen, H., Wang, Z., and Claudel, C. (2021). Skeleton-graph: Long-term 3d motion prediction from 2d observations using deep spatio-temporal graph cnns. *arXiv preprint arXiv:2109.10257*.

Nussbaumer, H. J. (1981). The fast fourier transform. In *Fast Fourier Transform and Convolution Algorithms*, pages 80–111. Springer.

Ragusa, F., Furnari, A., and Farinella, G. M. (2022). Meccano: A multimodal egocentric dataset for humans behavior understanding in the industrial-like domain.

Sofianos, T., Sampieri, A., Franco, L., and Galasso, F. (2021). Space-time-separable graph convolutional network for pose forecasting. *CoRR*, abs/2110.04573.

Vendrow, E., Kumar, S., Adeli, E., and Rezatofighi, H. (2022). Somoformer: Multi-person pose forecasting with transformers. *arXiv preprint arXiv:2208.14023*.

Yuan, Y. and Kitani, K. (2020). Dlow: Diversifying latent flows for diverse human motion prediction. In *European Conference on Computer Vision*, pages 346–364. Springer.

Zhang, J., Liu, H., Chang, Q., Wang, L., and Gao, R. X. (2020). Recurrent neural network for motion trajectory prediction in human-robot collaborative assembly. *CIRP annals*, 69(1):9–12.

Zhao, Z., Liu, Y., and Ma, L. (2022). Compositional action recognition with multi-view feature fusion. *Plos one*, 17(4):e0266259.

Zheng, Y., Yang, Y., Mo, K., Li, J., Yu, T., Liu, Y., Liu, C. K., and Guibas, L. J. (2022). Gimo: Gaze-informed human motion prediction in context. In *European Conference on Computer Vision*, pages 676–694. Springer.